ADVANCED MATERIALS

DOI: 10.1002/adma.200800918

Double Emulsion-Templated Nanoparticle Colloidosomes with Selective Permeability**

By *Daeyeon Lee* and *David A. Weitz**

Colloidosomes are microcapsules whose shell consists of densely packed colloidal particles. Their physical properties such as permeability, mechanical strength, and biocompatibility can be precisely controlled through the proper choice of colloids and preparation conditions for their assembly.[1–4] The high degree of control over their physical properties makes colloidosomes attractive structures for encapsulation and controlled release of materials ranging from fragrances and active ingredients to molecules produced by living cells.[5–7] The conventional approach to preparing colloidosomes involves two steps: first, colloidal particles are introduced into the continuous phase of a water-in-oil emulsion. The particles self-assemble at the interface between the two immiscible liquid phases and form a colloidal shell structure.[1,8] Subsequently, the colloidal shell structures, templated by the water droplets dispersed in the oil phase, are transferred to an aqueous phase either by centrifugation or repeated washing. This strategy has been used to create colloidosomes with particles ranging from 5 nm to several microns in diameter.[1,8–11] The colloidosome structures must be mechanically stabilized to successfully transfer them into an aqueous phase; however, even with this stabilization, the transfer processes are not efficient, often leading to damage of the original structure.[1,9,11,12] In addition, the size distribution of colloidosomes prepared by the conventional technique is rather broad, as polydisperse emulsions are typically used as templates. A narrow size distribution for colloidosomes is especially important for the encapsulation of active pharmaceutical ingredients where delivery of an exact amount is critical. Thus, it is important to develop a more convenient and direct means to create monodisperse and fully controllable colloidosomes, in particular, eliminating the transfer step.[13]

In this work, we demonstrate that nanoparticle colloidosomes with selective permeability can be prepared from monodisperse double emulsions as templates. Monodisperse water-in-oil-in-water (W/O/W) double emulsions with a core/shell geometry are generated using glass capillary microfluidic devices.[14] Hydrophobic silica nanoparticles dispersed in the oil shell stabilize the droplets and ultimately become the colloidosome shells upon removal of the oil solvent. The size of these double emulsions, and thus the dimensions of the resulting colloidosomes, can be precisely tuned by independently controlling the flow rates of each fluid phase.[14,15] Unlike the colloidosomes that are templated by water droplets in a continuous phase of oil, these colloidosomes are generated directly in a continuous phase of water; thus, there is no need to transfer the colloidosomes from an oil to an aqueous phase. Also, by incorporating different materials into the oil phase, it is possible to prepare composite colloidosomes. The thickness of the colloidosome shells, which is a critical parameter determining the mechanical strength and permeability of colloidosomes, can be controlled by changing the dimension of the double emulsion templates. These nanoparticle colloidosomes have selective permeability to molecules of different sizes, which is one of the hallmark characteristics of colloidosomes.[1,9] The permeability of low molecular weight molecules was investigated using fluorescence recovery after photobleaching (FRAP) method.[16,17] Our approach to prepare colloidosomes from W/O/W double emulsion templates provides a robust and general method to create monodisperse semipermeable nanoparticle colloidosomes with precisely tuned structure and composition.

Our microfluidic device combines a flow focusing and co-flowing geometry as schematically illustrated in Figure 1(a).[14] This geometry results in hydrodynamic flow focusing of three different fluid streams at the orifice of the collection tube and leads to the formation of double emulsions (see Supporting Information for a movie showing the formation of double emulsions from three fluid streams). We used water as inner and outer phases and a volatile organic solvent such as toluene or a mixture of toluene and chloroform as the middle phase. The double emulsions are stabilized by hydrophobic silica (SiO_2) nanoparticles, which are dispersed in the oil phase, without addition of surfactant. Without the nanoparticles, the double emulsions generated in the microcapillary devices are not stable. We believe that the double emulsions are stabilized by nanoparticles, which adsorb to the two oil/water interfaces. Such particle-stabilized emulsions have been extensively studied during the past century and are known as Pickering emulsions.[18,19] Other studies have also shown that nanoparticle colloidosomes can be created by the assembly of

[*] Prof. D. A. Weitz, Dr. D. Lee
School of Engineering and Applied Sciences and
Department of Physics
Harvard University
Cambridge, MA 02138 (USA)
E-mail: weitz@seas.harvard.edu

[**] This work was supported by the NSF (no. DMR-0602684) and the Harvard MRSEC (no. DMR-0213805). Hydrophobic silica nanoparticles were generously provided by Nissan Chemicals Inc. (Japan). We also thank Ho Cheung Shum and Rhutesh K. Shah for insightful discussion. Supporting Information is available online from Wiley InterScience or from the author.

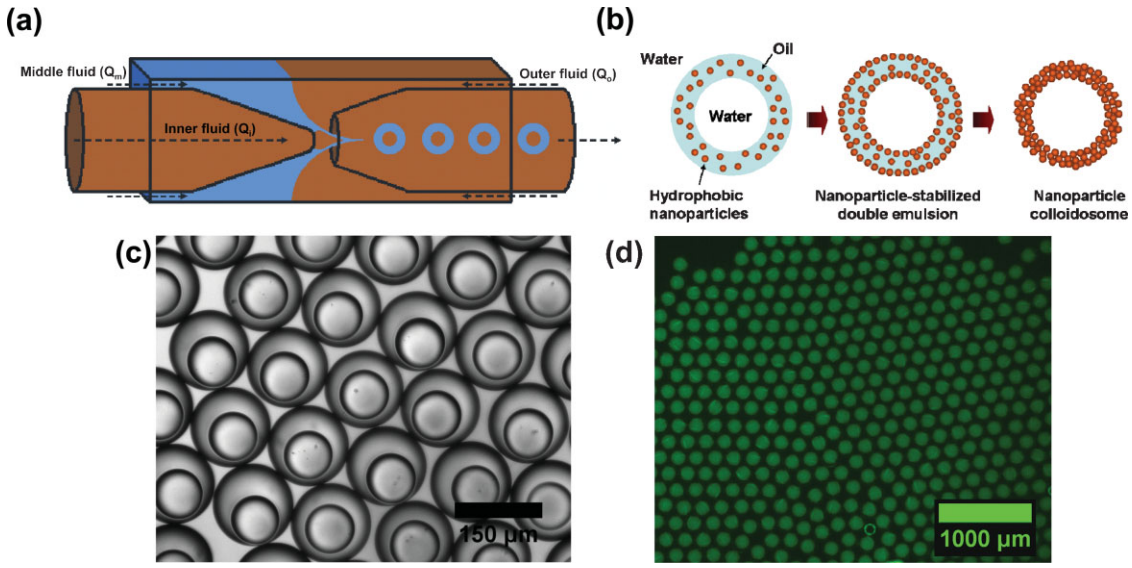

Figure 1. a) Schematic representation of microcapillary device for double emulsion generation. b) Schematic for the formation of nanoparticle colloidosomes from nanoparticle-stabilized water-in-oil-in-water double emulsions. Hydrophobic nanoparticles are suspended in the oil phase. Evaporation of oil phase leads to the formation of nanoparticle colloidosomes. c) Optical and d) fluorescence microscope images of double emulsions encapsulating 250 μg mL^{-1} FITC-dextran ($M_W = 70\,000$).

hydrophobic nanoparticles at water/oil interfaces.[3,8,9,11,20] After the nanoparticle stabilized double emulsions are collected, the oil phase is removed by evaporation, leading to the formation of nanoparticle colloidosomes through dense packing of nanoparticles as shown schematically in Figure 1(b).

The double emulsions generated from microcapillary devices are very monodisperse as evidenced by the hexagonal close packing of the drops, illustrated by optical and fluorescence microscopy images in Figure 1(c) and (d), respectively. These double emulsions can encapsulate molecules in the inner aqueous phase with essentially 100% efficiency. Such high encapsulation efficiency is possible since the drop formation process does not allow the inner aqueous phase to come in contact with the outer aqueous phase [Figure 1(a)]. Thus, as long as the encapsulated materials cannot permeate through the oil phase, essentially all of the molecules and materials can be retained within the interior of the drops. To illustrate this, we dissolve dextran labeled with fluorescein isothiocyanate (FITC-dextran) in the inner aqueous phase; it cannot be detected in the continuous outer phase, as seen in fluorescence microscope image in Figure 1(d).

One major advantage of using microcapillary devices to create the templates for colloidosome generation is in the precise control over the dimensions of the double emulsions; the size of inner drop (D_i) and outer drop (D_o), thus the thickness of oil shell ($H = (D_o - D_i)/2$), can be precisely and independently tuned by changing the flow rates (Q) of each phase.[14,15] For example, increasing the flow rate of the middle phase (Q_m) leads to the formation of drops with larger H and smaller D_i as illustrated in Figure 2(a). In contrast, increasing the flow rate of the inner phase (Q_i) results in formation of drops with larger D_i and smaller H as shown in Figure 2(b). Drops with smaller D_o and D_i, but with an approximately constant H, can be generated by increasing Q_o (flow rate of the outer phase) as shown in Figure 2(c) (see Supporting Information for images of double emulsions with different dimensions). Results from Figure 2(a) and (b) are summarized by plotting D_o/D_i as a function of Q_m/Q_i in Figure 2(d) and show good agreement with the predicted values [dotted line in Fig. 2(d)] estimated from

$$\frac{D_o}{D_i} = \left(1 + \frac{Q_m}{Q_i}\right)^{\frac{1}{3}} \quad (1)$$

The high degree of control over the drop dimensions afforded by our approach allows the fabrication of colloidosomes with precisely tuned structure; this is very difficult to achieve using the conventional technique of colloidosome formation.

Once the double emulsions are collected from the glass microcapillary device, nanoparticle colloidosomes are formed by removing the oil phase through evaporation [Fig. 1(b)]. A scanning electron microscopy (SEM) image of monodisperse colloidosomes prepared by evaporating toluene is shown in Figure 3(a) (See Supporting Information for an optical microscope image of colloidosomes). While colloidosomes with thin shells tend to collapse upon drying, those with thicker shells are able to structurally withstand the evaporation process and retain their spherical shape as shown in Figure 3(a). Close inspection of the colloidosome surfaces reveals wrinkles that resemble the herringbone buckling patterns observed in equibiaxially compressed stiff thin films atop elastomeric substrates.[21] In fact, these wrinkles develop

ADVANCED MATERIALS

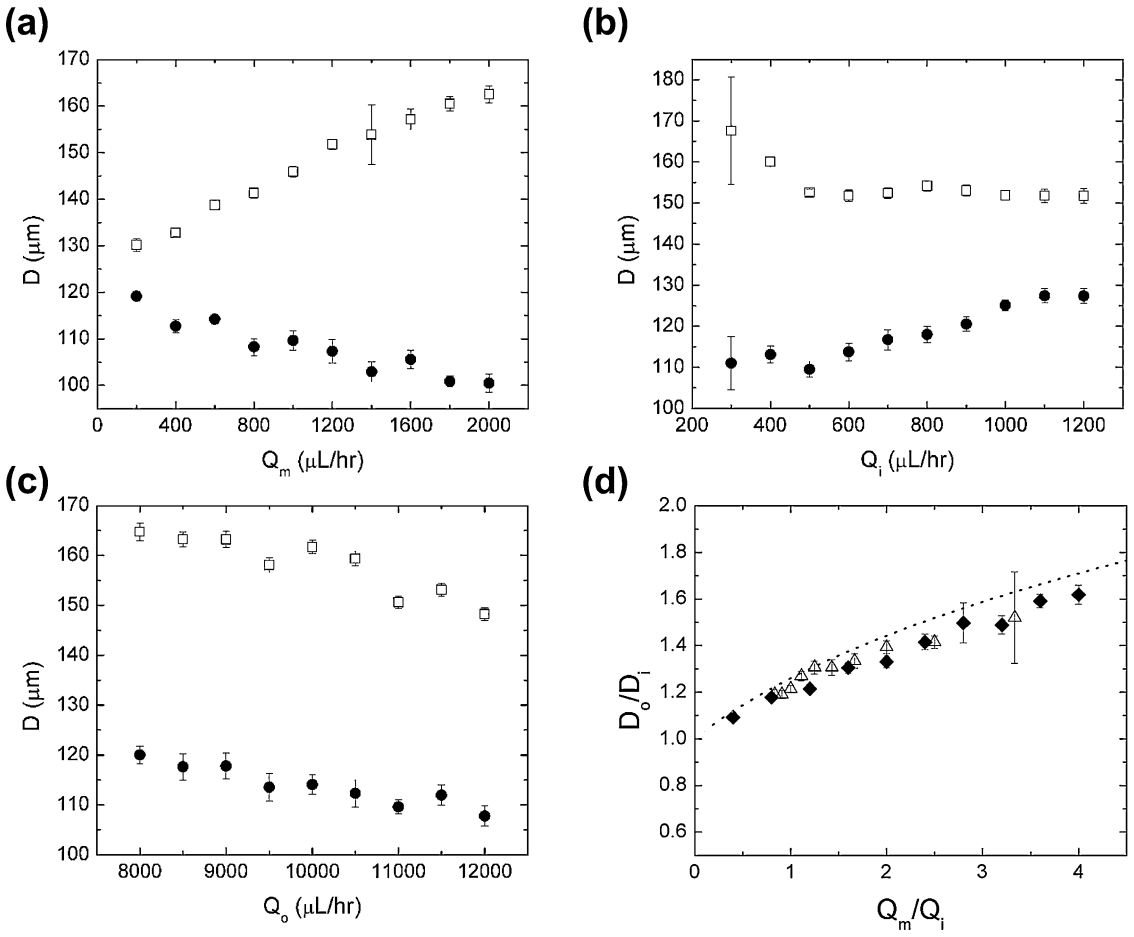

Figure 2. Effect of flow rates (Q) on the dimension of double emulsions. a) Flow rate of oil phase (Q_m) is varied while the flow rates of inner (Q_i) and outer phases (Q_o) were kept constant at 500 and 10 000 μL h^{-1}, respectively. b) Q_i is varied while Q_m and Q_o are kept constant at 1 000 and 10 000 μL h^{-1}, respectively. c) Q_o is varied while Q_m and Q_i are kept constant at 1 000 and 500 μL h^{-1}, respectively. Open squares and closed circles represent the diameters (D) of outer and inner drops, respectively, in (a) to (c). d) Plot of size ratio of outer to inner drop (D_o/D_i) versus flow rate ratio of middle to inner phase (Q_m/Q_i). Dotted line represents predicted values of D_o/D_i based on Equation 1. Closed diamonds and open triangles in (d) are data from (a) and (b), respectively. In all cases following solutions were used for each phase: outer phase = 2 wt % PVA in water, middle phase = 7.5 wt % silica nanoparticle in toluene and inner phase = 2 wt % PVA solution.

during evaporation of the oil phase. We believe that nanoparticles adsorbed to the water/toluene interface form a two-dimensional network and buckle during evaporation and shrinkage of the oil phase. Recently, it has been reported that nanoparticle monolayers with 60% surface coverage at water/air interface can buckle upon compression.[22]

Unlike colloidosomes that are prepared by the conventional technique, our approach provides a means to independently control the thickness of the shell of the colloidosomes; this is important in tuning their mechanical strength and permeability. The thickness and structure of colloidosome shells were observed by freeze-fracture cryogenic-SEM (cryo-SEM), which reveals that the shell thickness is highly uniform and defect free, as illustrated in Figure 3(b). We are able to create colloidosomes with shell thicknesses ranging from 100 nm to 10 μm by controlling the dimension of the double emulsions and the volume fraction of nanoparticles in the oil phase. A high magnification cryo-SEM image shows that the nanoparticles are randomly and densely packed to form the shell of the colloidosome (see Supporting Information).

In addition to nanoparticle colloidosomes, our approach enables the preparation of multicomponent colloidosomes, or composite microcapsules. For example, by dissolving poly-(D,L-lactic acid) (PLA), which is a biodegradable polymer, in the oil phase containing hydrophobic silica nanoparticles, we are able to prepare PLA/SiO_2 composite microcapsules as seen in Figure 3(c). The thickness of the composite capsule shell is approximately 200 nm as shown in the inset of Figure 3(c); this is in excellent agreement with the estimate of 220 nm based on the volume fraction of solid materials (10 vol %) in the oil phase. Magnetically responsive composite colloidosomes can also be prepared by suspending Fe_3O_4 magnetic nanoparticles along with hydrophobic silica nanoparticles in the oil phase. These magnetic colloidosomes can be separated from the solution using a magnetic field as shown in Figure 3(d). These examples demonstrate that it is straightforward to fabricate

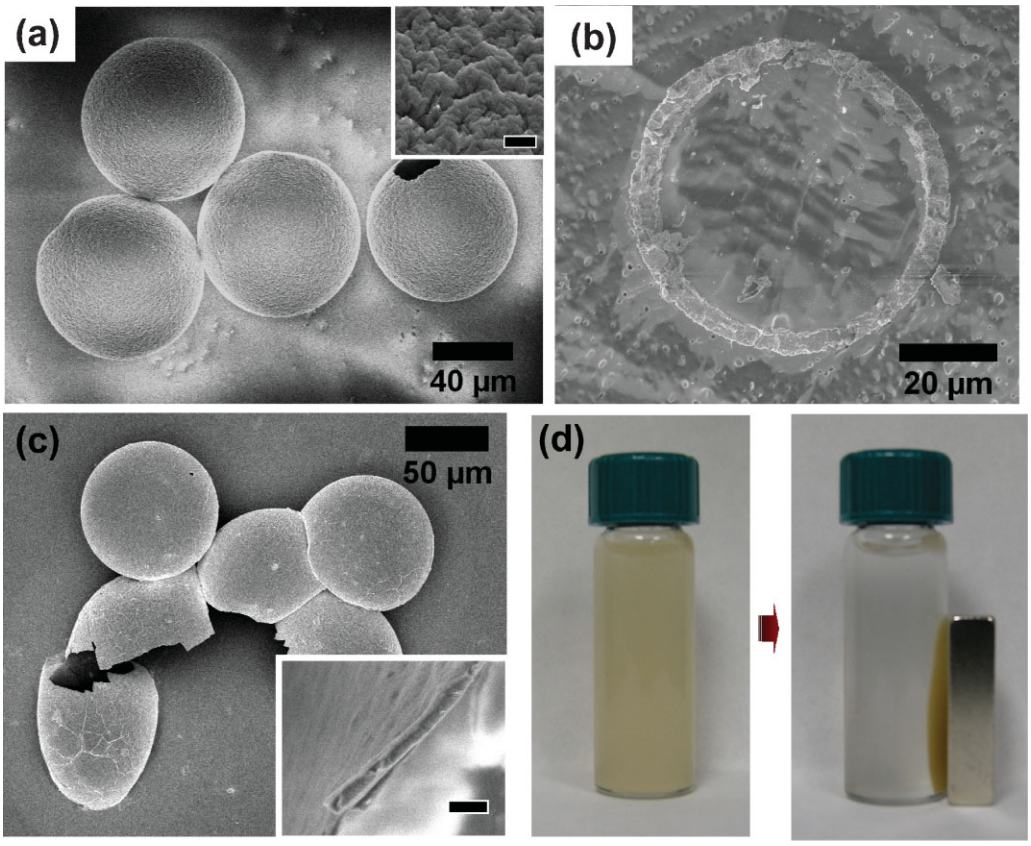

Figure 3. a) SEM image of nanoparticle colloidosomes dried on a substrate. Inset is a high magnification image of colloidosome surface (scale bar = 600 nm). b) Cross-section of a colloidosome obtained with freeze-fracture cryo-SEM. c) SEM image of PLA/SiO_2 composite capsules dried on a substrate. Inset shows the cross-section of a broken capsule shell (scale bar = 500 nm). d) Photo images demonstrating the magnetic separation of 10 nm Fe_3O_4 nanoparticle containing colloidosomes.

composite colloidosomes with precisely tuned composition; this is difficult to achieve using other methods.

A hallmark of colloidosomes is their selective permeability.[1,9] Since colloidosomes are made from colloidal particles, their shells are intrinsically porous due to the presence of interstitial voids between the packed particles. The selective permeability of these colloidosomes is demonstrated by exposing them to aqueous solutions of fluorescence probes with different molecular weights. The permeation of fluorescence probes into the interior of the colloidosomes is detected by confocal laser scanning microscopy (CLSM). Calcein, a low molecular weight ($M_w = 622.55$) fluorescent molecule, freely diffuses into the interior of SiO_2 nanoparticle colloidosomes as shown in Figure 4(a). In contrast, FITC-dextran, a high molecular weight polymer ($M_w \sim 2\,000\,000$), cannot diffuse into the interior of the colloidosomes [Figure 4(b)]. The striking difference in the permeability is due to size exclusion and clearly demonstrates the selective permeability of these colloidosomes. The pore size of randomly closed packed spheres is approximately 10% of the radius.[23] Therefore, calcein whose size is less than 1 nm [24] can diffuse into the colloidosomes without much resistance as the size of nanoparticles used for their fabrication is $10 \sim 20$ nm. In contrast, it is very difficult for the high molecular weight dextran, whose radius of gyration is ~40 nm, to diffuse through the shell of the colloidosomes.[25] The diffusion of calcein can, however, be completely prevented by incorporating a polymer such as PLA, into the colloidosome structures as illustrated by colloidosomes with dark interiors in Figure 4(c). These composite colloidosomes remained impermeable to calcein at least for 24 h. The polymer fills the interstices between the nanoparticles making the composite capsules essentially impermeable. These results demonstrate that the shells of nanoparticle colloidosomes are porous and that colloidosomes exhibit selective permeability; moreover, by incorporating polymers into the colloidosomes, the permeability of small molecular weight molecules can be drastically reduced. The size of the pores in the colloidosome shells is proportional to the size of nanoparticles used;[23] therefore, the selectivity of the colloidosomes can be controlled by changing the size of the nanoparticles.

Quantitative information on the permeability of colloidosomes is important for a number of applications including controlled release of fragrances, pesticides, and pharmaceuticals. We utilize FRAP to measure the permeability of a low molecular weight probe, 5(6)-carboxyfluorescein (CF). CF was

ADVANCED MATERIALS

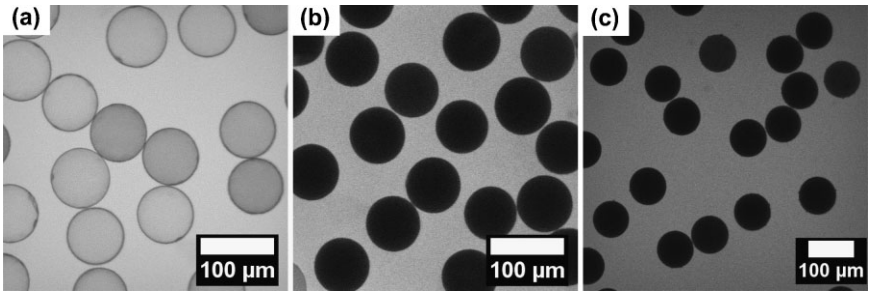

Figure 4. Confocal laser scanning microscope images demonstrating semipermeability of nanoparticle colloidosomes. a) Low molecular weight fluorescence probe, calcein and b) high molecular weight probe, FITC-dextran ($M_W \sim 2\,000\,000$) was added to the continuous phase. c) PLA/SiO_2 nanocomposite microcapsules completely prevent the permeation of calcein into the interior of the colloidosomes. In all cases, the images were taken ~30 min after the addition of probe molecules.

allowed to permeate into the colloidosomes and then the laser was focused in the interior region of colloidosome, photobleaching the CF that was trapped in the interior. The gradual recovery of fluorescence as a function of time due to the diffusion of unbleached ''fresh'' probes into the colloidosome is seen in Figure 5. The temporal evolution of the recovery of fluorescence intensity within a capsule can be described by:[16,17]

$$\frac{I(t)}{I_\infty} = 1 - e^{-At} \tag{2}$$

where, $A = 3P/r$. P is the permeability of the probe through the colloidosome shell and r is the radius of the colloidosome. $I(t)$ and I_∞ represent the intensity of fluorescence probe within colloidosomes at time t and $t \to \infty$, respectively, assuming that

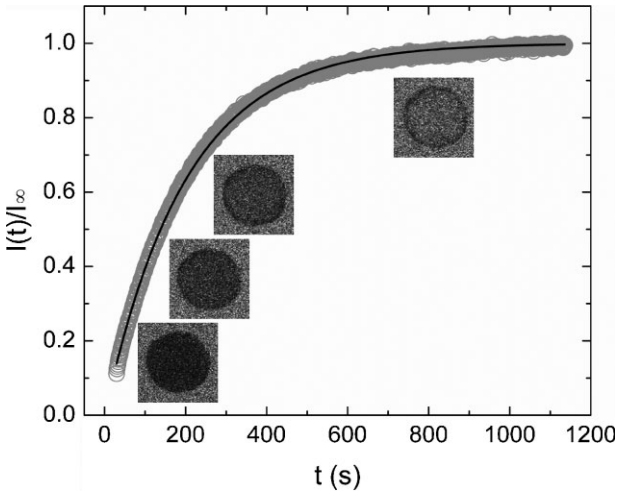

Figure 5. FRAP of CF to determine the permeability of nanoparticle colloidosome. Open circles represent FRAP curve and the solid curve is based on Equation 2. Fluorescence images of a nanoparticle colloidosome (52 μm in diameter) during FRAP experiment are shown in the graph. The permeability of this particular example is 0.044 μm s^{-1}. I_∞ refers to the intensity of the CF within the colloidosome at $t = \infty$.

complete photobleaching is achieved at $t = 0$. Using Equation 2, the permeability of CF across nanoparticle colloidosome shell is determined to be 0.062 ± 0.028 μm s^{-1}. Since diffusivity is the product of permeability (P) and the thickness of the shell, the value of permeability can be converted to the diffusion coefficient of CF molecules across the nanoparticle colloidosome; thus, the diffusion coefficient of the probe is estimated to be 3.7×10^{-2} μm^2 s^{-1}. This value of diffusivity of CF is a few orders of magnitude greater than the diffusivity of similar probes through widely studied polyelectrolyte hollow microcapsules that are generated by layer-by-layer (LbL) assembly of oppositely charged polyelectrolytes.[17,26] This result is not surprising considering that the LbL microcapsule shells consist of polymers that are highly crosslinked by electrostatic interactions whereas the colloidosome shells are more porous.

In this work, we have demonstrated that semipermeable colloidosomes comprising nanoparticles and other materials including polymers can be prepared from water-in-oil-in-water (W/O/W) double emulsions. Our approach provides a general and robust method to generate monodisperse nanoparticle colloidosomes and composite microcapsules. By controlling the size of nanoparticles, it will be possible to control the selectivity as well as the permeability of nanoparticle colloidosomes making them attractive means to encapsulate active ingredients, drugs, and food ingredients for applications in controlled release and drug delivery.

Experimental

Materials: Glass microcapillaries were purchased from World Precision Instruments, Inc. and Atlantic International Technologies, Inc. Hydrophobic silica nanoparticles suspended in toluene were generously provided by Nissan Chemical Inc. (Japan). Toluene, calcein, CF, FITC-labeled dextran ($M_w \sim 2\,000\,000$ and 70 000) and polyvinyl alcohol (PVA; 87 ~ 89% hydrolyzed, $M_w = 13000 \sim 23\,000$) were obtained from Sigma–Aldrich. PLA (PLA; $M_w \sim 6\,000$–$16\,000$, polydispersity index (PDI) = 1.8) was obtained from Polysciences. Magnetic nanoparticles (10 nm) suspended in toluene were purchased from NN Labs, LLC. Chemicals were used as received without further purification.

Microcapillary Device Fabrication and Generation of Double Emulsions: The detailed preparation of glass microcapillary devices was described previously [14]. Briefly, cylindrical glass capillary tubes with an outer diameter of 1 mm and inner diameter of 580 μm were pulled using a Sutter Flaming/Brown micropipette puller. The dimension of tapered orifices was adjusted using a microforge (Narishige, Japan). Typical dimensions of orifice for inner fluid and collection were $10 \sim 50$ and $30 \sim 500$ μm, respectively. The orifice sizes can be adjusted with the puller and the microforge to control the dimensions of double emulsions. The glass microcapillary tubes for inner fluid and collection were fitted into square capillary tubes that had an inner dimension of 1 mm. By using the cylindrical capillaries whose outer diameter are the same as the inner dimension of the square tubes, a good alignment could be easily achieved to form a coaxial geometry. The distance between the tubes for inner fluid and collection was adjusted to be $30 \sim 150$ μm [Figure 1(a)]. A transparent epoxy resin was used to seal the tubes where required. Solutions were delivered to the microfluidic device through polyethylene tubing (Scientific Commodities) attached to syringes (Hamilton Gastight or SGE) that were driven by positive displacement syringe pumps (Harvard Apparatus, PHD 2000 series). The drop formation was monitored with a high-speed camera (Vision Research) attached to an inverted microscope.

For the generation of W/O/W double emulsions, three fluid phases are delivered to the glass microcapillary devices. The outer and inner aqueous phases comprise PVA solution (outer phase $= 0.2 \sim 2$ wt % and inner phase $= 0 \sim 2$ wt %). The middle phase typically consists of ca. 7.5 wt % hydrophobic silica nanoparticles suspended in toluene. The concentration of nanoparticles in the middle phase was varied between 3 and 22 wt %. PLA/SiO_2 nanoparticle composite microcapsules were prepared by adding PLA and silica nanoparticles to toluene at a concentration of 50 mg mL^{-1} and 7.5 wt %, respectively. Magnetically responsive colloidosomes were prepared by mixing silica nanoparticle suspension (45 wt % in toluene), magnetic nanoparticle suspension (10 nm in diameter, 2 mg mL^{-1} in toluene) and toluene in a 1:4:1 volumetric ratio.

To convert double emulsion droplets to nanoparticle colloidosomes, the emulsion was exposed to vacuum overnight. The nanoparticle colloidosomes were then washed with a copious amount of deionized water to remove the remaining oil phase. SEM was performed on a Zeiss Ultra55 field emission scanning electron microscope (FESEM) at an acceleration voltage of 5 kV. Samples were coated with approximately $5 \sim 10$ nm of gold. Freeze-fracture cryo-SEM was performed on a Dual Beam 235 focused ion beam (FIB)-SEM at an acceleration voltage of 5 kV. A small aliquot of sample was placed on a sample stub and was plunged into liquid nitrogen. The frozen sample was fractured using a sharp blade and coated with a thin layer of Au before imaging.

Permeability Measurement Via Fluorescence Recovery After Photobleaching (FRAP): A small volume (~50 μL) of NP colloidosome suspension was place in an elastomer isolation chamber atop a glass coverslide. The colloidosomes were allowed to sediment to the bottom of the chamber for 30 min before FRAP experiments. FRAP was performed using Leica TCS SP5 confocal microscope. Ar laser at a wavelength of 488 nm was used at maximum intensity to photobleach the dyes, and the recovery was observed at 1% of the bleaching intensity at $1 \sim 2$ s intervals.

Received: April 4, 2008
Revised: May 14, 2008
Published online: August 11, 2008

[1] A. D. Dinsmore, M. F. Hsu, M. G. Nikolaides, M. Marquez, A. R. Bausch, D. A. Weitz, *Science* **2002**, *298*, 1006.
[2] S. Shilpi, A. Jain, Y. Gupta, S. K. Jain, *Crit. Rev. Ther. Drug* **2007**, *24*, 361.
[3] A. Boker, J. He, T. Emrick, T. P. Russell, *Soft Matter* **2007**, *3*, 1231.
[4] D. Y. Wang, H. W. Duan, H. Möhwald, *Soft Matter* **2005**, *1*, 412.
[5] A. Madene, M. Jacquot, J. Scher, S. Desobry, *Int. J. Food Sci. Technol.* **2006**, *41*, 1.
[6] R. Langer, *Nature* **1998**, *392*, 5.
[7] B. F. Gibbs, S. Kermasha, I. Alli, C. N. Mulligan, *Int. J. Food Sci. Nutr.* **1999**, *50*, 213.
[8] Y. Lin, H. Skaff, T. Emrick, A. D. Dinsmore, T. P. Russell, *Science* **2003**, *299*, 226.
[9] H. W. Duan, D. Y. Wang, N. S. Sobal, M. Giersig, D. G. Kurth, H. Möhwald, *Nano Lett.* **2005**, *5*, 949.
[10] Y. Lin, A. Boker, H. Skaff, D. Cookson, A. D. Dinsmore, T. Emrick, T. P. Russell, *Langmuir* **2005**, *21*, 191.
[11] H. Skaff, Y. Lin, R. Tangirala, K. Breitenkamp, A. Boker, T. P. Russell, T. Emrick, *Adv. Mater.* **2005**, *17*, 2082.
[12] Y. Lin, H. Skaff, A. Boker, A. D. Dinsmore, T. Emrick, T. P. Russell, *J. Am. Chem. Soc.* **2003**, *125*, 12690.
[13] A. B. Subramaniam, D. Gregory, J. Petkov, H. A. Stone, *Phys. Chem. Chem. Phys.* **2007**, *9*, 6476.
[14] A. S. Utada, E. Lorenceau, D. R. Link, P. D. Kaplan, H. A. Stone, D. A. Weitz, *Science* **2005**, *308*, 537.
[15] L. Y. Chu, A. S. Utada, R. K. Shah, J. W. Kim, D. A. Weitz, *Angew. Chem. Int. Ed.* **2007**, *46*, 8970.
[16] Z. H. An, H. Möhwald, J. B. Li, *Biomacromolecules* **2006**, *7*, 580.
[17] G. Ibarz, L. Dahne, E. Donath, H. Möhwald, *Chem. Mater.* **2002**, *14*, 4059.
[18] S. U. Pickering, *J. Chem. Soc.* **1907**, *91*, 2001.
[19] B. P. Binks, *Curr. Opin. Colloid Interface* **2002**, *7*, 21.
[20] Y. J. He, S. T. Qi, S. Y. Zhao, *Prog. Chem.* **2007**, *19*, 1443.
[21] X. Chen, J. W. Hutchinson, *Scr. Mater.* **2004**, *50*, 797.
[22] M. K. Bera, M. K. Sanyal, S. Pal, J. Daillant, A. Datta, G. U. Kulkarni, D. Luzet, O. Konovalov, *Europhys. Lett.* **2007**, *78*, 56003.
[23] M. D. Rintoul, S. Torquato, *Phys. Rev. E* **1998**, *58*, 532.
[24] The size of calcein was estimated using an online cheminformatics software, http://www.molinspiration.com/.
[25] C. E. Ioan, T. Aberle, W. Burchard, *Macromolecules* **2000**, *33*, 5730.
[26] A. A. Antipov, G. B. Sukhorukov, E. Donath, H. Möhwald, *J. Phys. Chem. B* **2001**, *105*, 2281.

